DOI: 10.5505/2023geoteknik.SS-10

# SOIL LIQUEFACTION MANIFESTATIONS AT HATAY AIRPORT AFTER THE FEBRUARY 6 KAHRAMANMARAŞ EARTHQUAKE SEQUENCE

## HATAY HAVALİMANI'NDA 6 ŞUBAT KAHRAMANMARAŞ DEPREMLERİ SONRASINDA GÖZLEMLENEN ZEMİN SIVILAŞMASI BELİRTİLERİ

**Elife Cakir[1], Kemal Onder Cetin[2], Yalçın Eyigün[3], and Candan Gokceoglu[4]**

## ABSTRACT

The performance of the Hatay Airport is investigated from seismic soil liquefaction engineering perspective. The Airport was shaken by the M7.8 and M7.6 Pazarcık and Ekinözü-Elbistan Kahramanmaraş earthquake sequence. This paper presents i) the seismic response of the Hatay Airport, more specifically, the surface manifestation of seismic soil liquefaction in the form of soil ejecta, ii) the results of site investigation studies, performed prior to the events, and iii) the assessments of soil liquefaction triggering. The case history performance documented herein, and the assessment results are believed to be useful in the development of case history-based predictive models for the assessment of liquefaction triggering and post-liquefaction ground deformations.
***Keywords:*** *Ejecta, High plasticity clay, Kahramanmaraş earthquake, Liquefaction*

## ÖZET

6 Şubat 2023'te Kahramanmaraş Pazarcık ve Kahramanmaraş Ekinözü-Elbistan'da moment büyüklükleri 7.8 ve 7.6 olan iki deprem meydana gelmiştir. Bu depremler sırasında Hatay Havalimanı'nda gözlenen sismik zemin sıvılaşması irdelenmiştir. Bildiri kapsamında, i) havalimanında görülen sismik zemin fışkırmaları, ii) zemin araştırma sondaj çalışmaları ve iii) zemin sıvılaşması tetiklenme analizleri tartışılmıştır. Bildiride sunulan vaka analizi ve değerlendirme sonuçlarının, sıvılaşma tetiklenmesi ve deformasyonlarının belirlenmesine yönelik tahmin modellerinin geliştirilmesine yardımcı olacağı düşünülmektedir.
***Anahtar kelimeler:*** *Kahramanmaraş depremleri, Sıvılaşma, Yüksek plastisiteli kil, Zemin fışkırması*

## 1. INTRODUCTION

On February 6, 2023, two earthquakes, with moment magnitudes of M7.8 and M7.6, occurred in Kahramanmaraş-Türkiye on the East Anatolian Fault zone. The first event occurred at 04:17 local time, followed by a second earthquake at 13:24 local time. After the mainshocks, more than ten thousand earthquakes were recorded from February 6 to March 1, within 200 km radii from the event epicenters.

[1]Graduate Student, Middle East Technical University, Faculty of Engineering, Department of Civil Engineering, cakire@metu.edu.tr (corresponding author)
[2] Prof. Dr., Middle East Technical University, Faculty of Engineering, Department of Civil Engineering, ocetin@metu.edu.tr
[3] Dr., İstanbul Ticaret University, Faculty of Engineering, Department of Civil Engineering, yeyigun@ticaret.edu.tr
[4] Prof. Dr., Hacettepe University, Faculty of Engineering, Department of Geological Engineering, cgokce@hacettepe.edu.tr

Among these aftershocks, more than 400 of them had magnitudes equal to or greater than 5.0. Figure 1 shows the spatial distribution of the mainshocks and aftershocks, along with their induced fault rupture patterns along with strong ground motion stations (SGMS). The epicenter of the first event, which has a focal depth of 8.6 km, is located at 37.288°N and 37.043°E (AFAD, the national disaster and emergency management agency), close to Kahramanmaraş-Pazarcık. The second event has a focal depth of 7.0 km, and its epicenter is located in Kahramanmaraş-Elbistan-Ekinözü, at 38.089°N, 37.239°E (AFAD).

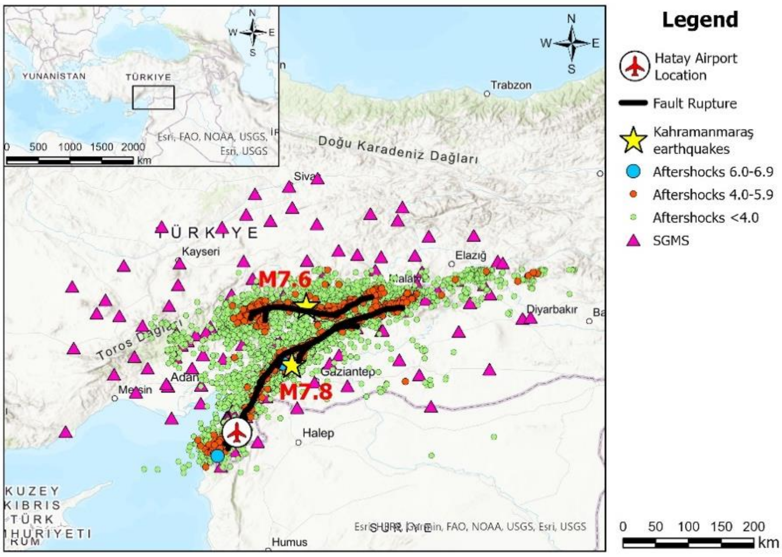


Figure 1. The spatial distribution of mainshocks and aftershocks (as of March 1, 2023) along with the induced fault rupture due to the Türkiye-Kahramanmaraş-Pazarcık and -Ekinözü-Elbistan earthquake sequence

This paper presents a preliminary study on the observed liquefaction surface manifestations at the Hatay Airport located in Antakya, Hatay. The study presents the results of site investigations and laboratory tests. These site investigations and laboratory test results serve as the basis for evaluating the soil liquefaction susceptibility and triggering.

## 2. SITE DESCRIPTION AND SEISMOTECTONIC SETTINGS

Hatay Airport, which has been in service since 2007, is located in the city of Hatay. It is approximately 20 km north of the Antakya district and 25 km south-east of the İskenderun. The Airport was built on former Lake Amik. Starting in the 1940's, Lake Amik gradually transformed into a plain after draining the lake to the Asi (Orontes) river to increase agriculture production capacity (Kilic et al., 2006). In addition to its agricultural potential, the basin is also unique for its tectonic features. It is located within the triple junction of the Arabian, and African plates and the Anatolian Block. Three regional scale tectonic structures, namely, the North trending Dead Sea Fault (DSF), North-East trending East Anatolian Fault (EAF), and North-East trending Cyprus Arc (CA) (Mahmoud et al., 2013; Yuce et al., 2014) cross the region.

## 3. STRONG GROUND MOTIONS RECORDED DURING THE 2023 KAHRAMANMARAŞ EARTHQUAKE SEQUENCE

AFAD operates 1548 strong ground motion stations nationwide. 379 and 244 of these stations were triggered during the Pazarcık M7.8 and Ekinözü-Elbistan earthquakes, respectively. These stations are shown by pink triangles in Figure 1. Figure 2 presents the attenuation of the recorded PGA intensities with Joyner and Boore distance, $R_{jb}$, during both events. The Hatay Airport is located approximately 300 m away from the fault rupture of the Pazarcık event and 200 km away from the fault rupture of the Ekinözü-Elbistan event. The PGA values corresponding to the $R_{jb}$ distances at soil sites (i.e.: $V_{S30}$=180-360 m/s) are estimated as 0.56 g and in the range of 0.02 to 0.03 g for the Pazarcık and Ekinözü-Elbistan events, respectively. Consistently, it was concluded that the Ekinözü-Elbistan event did not produce significant shaking levels at the site. Therefore, the assessments of liquefaction triggering are performed for the Pazarcık event. $PGA_{rock}$ value at the site location with a $V_{S30}$ 760-1500 m/s (i.e.: a rock site) is estimated to vary in the range of 0.37 and 0.70 g, as illustrated in Figure 2. On the basis of Seed et al. (2001) site classification scheme, the site is categorized as a class E site. The same study suggests a PGA value of 0.39 and 0.50 g, respectively, for a class E site. Consistently, the site and event-specific PGA level at the Hatay Airport site is estimated as 0.55 g.

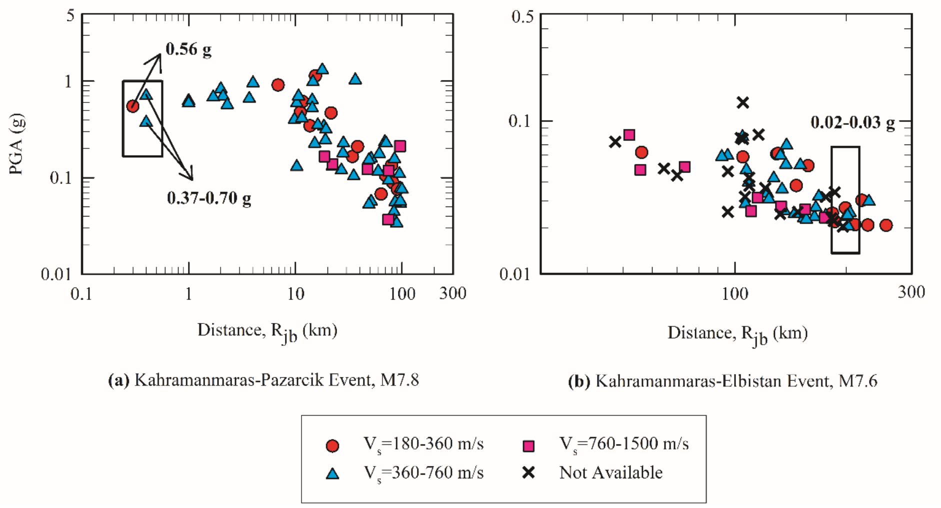


Figure 2. Joyner and Boore distance attenuation of PGA's recorded during a) Pazarcık and b) Ekinözü-Elbistan event

## 4. SITE INVESTIGATIONS AND OBSERVED SOIL LIQUEFACTION MANIFESTATIONS

A series of site investigation studies in the form of borings, disturbed and undisturbed sampling, in-situ (pressuremeter and standard penetration test, SPT), and laboratory (soil classification, triaxial tests, etc.) tests were performed during the engineering design stage of the Airport. The lithological unit in the study area is Quaternary alluvium, which consists of sandy and silty clayey soils. The field Standard Penetration Test blow counts (SPT-N) were reported in the range of 2-18. The site was accessed three days after the earthquake sequence, on February 9, 2023. The surface manifestations of soil liquefaction in the form of soil ejecta were observed. Figure 3 presents sample pictures illustrating soil ejecta and their locations. The terminal building was designed and constructed to be on piled foundations. Hence, it did not suffer from liquefaction triggering and induced bearing capacity problems, and/or displacements and deformations. Liquefaction manifestation was observed mostly in the free field away from the structures where ground improvement or reinforcement was not performed.


Figure 3. Locations of the soil ejecta and sample pictures

## 5. SEISMIC SOIL LIQUEFACTION ENGINEERING ASSESSMENTS

As part of soil liquefaction engineering evaluations, the analyses for susceptibility and triggering were performed. The assessments focused on the region, where liquefaction surface manifestations were mapped. The boreholes S5, S8, and S11 which were drilled during the planning stage, were used for the purpose.

### 6.1. Liquefaction Susceptibility Assessments

The liquefaction ejecta samples were retrieved at five locations, shown in yellow font in Figure 3. These samples were tested in conformance with ASTM D7928-17 and ASTM D6913/ D6319M-17 standards to assess their grain size characteristics and ASTM D4318-10e1 standard to assess their consistency limits. In Figure 4, their grain size distribution curves are comparatively presented with the grain size range of liquefaction susceptible soils, recommended by Tsuchida (1970). The ejecta sample grain size distribution curves fall in the range of liquefaction-susceptible soils. The grain size distribution characteristics are summarized in Table 1. Based on the Unified Soil Classification System (USCS) (ASTM D2487-17e1), the soil ejecta samples are classified as clayey sand (SC), silty sand (SM), low plasticity clay (CL), and unexpectedly, high plasticity clay (CH).

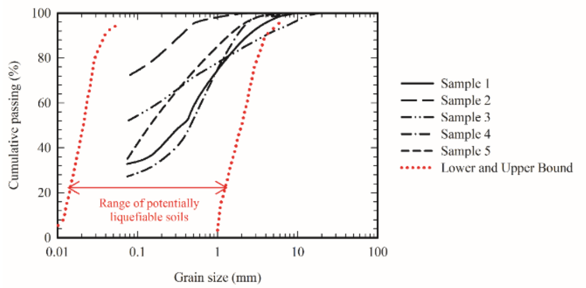


Figure 4. Grain size distribution of the soil ejecta

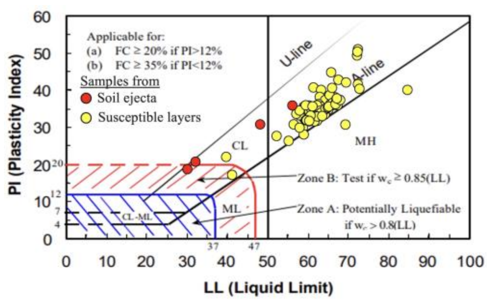


Figure 5. Liquid limit and plasticity index values of fine-grained soil samples on Seed et al. (2003) liquefaction susceptibility chart

Additionally, Figure 5 presents the consistency limits of soil ejecta samples along with the ones of the samples retrieved from the susceptible soil layers. The site investigation studies show that the site is composed of low to high plasticity clays, with minor silty and sandy lenses. Samples 2 and 3 confirm the presence of low to high plasticity ejecta; hence even though it is not in conformance with the current state of knowledge, they are assumed to be susceptible to liquefaction, and triggering assessments will be performed for these CL and CH type soils.

Table 1. Grain size distribution, consistency limits, and soil classification of ejecta

| Sample ID | Gravel (%) | Sand (%) | Fines (%) | LL (%) | PL (%) | PI (%) | Soil type |
|---|---|---|---|---|---|---|---|
| Sample 1 | 3.0 | 64.2 | 32.8 | 32 | 11 | 21 | SC |
| Sample 2 | 0.0 | 28.4 | 71.6 | 56 | 20 | 36 | CH |
| Sample 3 | 8.5 | 39.7 | 51.8 | 48 | 17 | 31 | CL |
| Sample 4 | 1.5 | 71.3 | 27.2 | 30 | 11 | 19 | SC |
| Sample 5 | 0.7 | 64.4 | 34.9 | - | - | - | SC-SM |

**6.2. Likelihood of Liquefaction Triggering**

Seismic soil liquefaction triggering evaluations were performed for boreholes S5, S8, and S11. During the assessments, the earthquake-induced cyclic stress ratios (CSR) were evaluated closely following the simplified procedures (Seed and Idris, 1971). Due to the low to high plasticity and clayey nature of the ejecta soil, currently available liquefaction-triggering predictive methodologies, developed for mostly non-plastic soils, could not be directly used. Hence, the results are only shown in the CSR vs. $N_{1,60}$ domain along with the boundary curves of non-plastic soils, for only comparison purposes. As discussed earlier in Section 3, the site-specific PGA value is adopted as 0.50 g. Figure 6 presents the soil type, including overburden, equipment, and procedure-corrected SPT $N_{1,60}$ values along with cyclic stress ratio values. The CSR values were estimated at each SPT depth by using simplified procedures along with Cetin and Seed's (2004) shear mass participation factors ($r_d$). In estimating $r_d$, the shear wave velocity value representing the upper 12 m (i.e.: $V_{S12}$) is adopted as 120 m/s. In Figure 6, pink-shaded soil layers are identified as the suspect liquefied layers, selected to have similar characteristics to the surface ejecta. The soil ejecta, entitled "Sample 1, 2 and 4" is located nearby borehole S8. Hence, consistent with the analysis results, the soft CH layer present in the soil profile at S8 is concluded as the suspect liquefied layer. The location of "Sample 3" and "Sample 5" are located nearby the boreholes S5 and S7, respectively. Again, the CH layer was identified as the origin of the ejecta and the suspect liquefied layer.

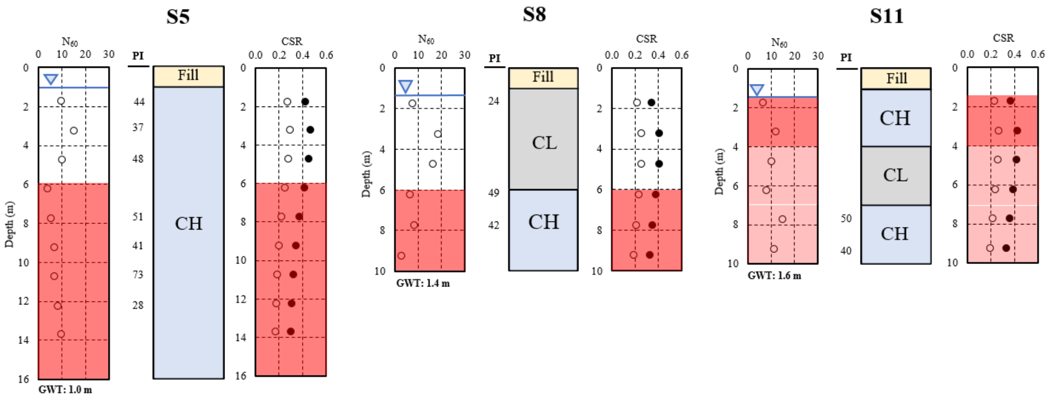


Figure 6. Assessed borelogs from the site where liquefaction surface manifestations were observed

The analysis results are shown in the normalized cyclic stress ratio CSR vs. SPT N  domain along with the Cetin et al. (2018) liquefaction triggering boundary curves. In this figure, red balls represent the liquefied suspect CH and CL layers. The predicted liquefaction trigger performances by Cetin et al. (2018) methodology are only presented to provide a visual comparison. It is noted that currently, available liquefaction triggering boundary curves are not suitable to assess the liquefaction response of low to high plasticity clays at the site.

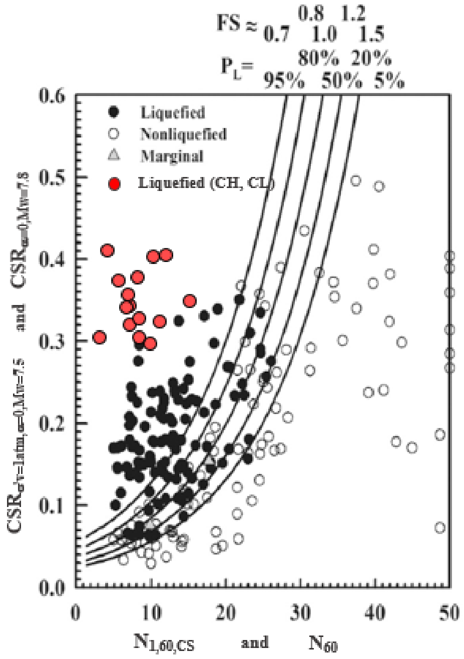


Figure 7. Liquefaction triggering assessment results as compared with the database and boundary curves of Cetin et al. (2018)

## 6. SUMMARY AND CONCLUSIONS

On February 6, 2023, Pazarcık and Ekinözü-Elbistan earthquakes with M7.8 and M7.6 occurred in Kahramanmaraş-Türkiye. After the mainshocks, more than ten thousand earthquakes were recorded from February 6 to March 1, within a 200 km radius of the event epicenters. More than ten cities, Kahramanmaraş, Adıyaman, Hatay, Osmaniye, Gaziantep, Kilis, Şanlıurfa, Diyarbakır, Malatya, Adana, and Elazığ have been affected greatly by this earthquake sequence. This paper presents a preliminary study on the observed liquefaction surface manifestations at the Hatay Airport located in Antakya-Hatay. The study involves the presentation of site investigations and laboratory test results. They serve as the basis for evaluating the soil liquefaction triggering. A series of site investigation studies in the form of borings, disturbed and undisturbed sampling, in-situ (pressuremeter and standard penetration test, SPT), and laboratory (soil classification, triaxial tests, etc.) tests were performed during the engineering design stage of the Airport. The lithological unit in the study area is Quaternary alluvium, which consists of sandy and silty clayey soils. The analyses for liquefaction susceptibility and triggering were performed based on the site investigation data. Rather unexpectedly with available literature and consistent with surface ejecta, CH layers are concluded to be the suspect liquefied layer. It is hoped that the data and results presented herein will contribute to the further development and refinement/calibration of increasingly accurate and reliable empirical and/or analytical methods for assessing hazards due to the triggering of liquefaction and consequent liquefaction-induced ground deformations and displacements.

## REFERENCES

ASTM D2487-17e1. Standard practice for classification of soils for engineering purposes (Unified Soil Classification System), West Conshohocken, PA 2017.

ASTM D4318-10e1 (2010) Standard test methods for liquid limit, plastic imit, and plasticity index of soils. ASTM International, West Conshohocken, PA.

ASTM D6913/D6319M-17. Standard test method for particle-size distribution (gradation) of soils using sieve analysis. West Conshohocken, PA 2017.

ASTM D7928-17. Standard test method for particle-size distribution (gradation) of fine-grained soil using the sedimentation (hydrometer) analysis. West Conshohocken, PA 2016.

Cetin KO and Seed RB. Nonlinear shear mass participation factor, $r_d$ for cyclic shear stress ratio evaluation. Journal of Soil Dynamics and Earthquake Engineering 2004;24(2):103-113.

Cetin KO, Seed R, Kayen R, Moss R, Bilge H, Ilgac M, Chowdhury K. SPT-based probabilistic and deterministic assessment of seismic soil liquefaction triggering hazard. Soil Dynamics and Earthquake Engineering 2018;115:698-709. https://doi.org/10.1016/j.soildyn.2018.09.012

Kilic, S., Evrendilek, F., Berberoglu, S. & Demirkesen, A. C. (2006). Environmental monitoring of land-use and land-cover changes in Amik Plain, Turkey. Environmental Monitoring and Assessment 2006;114:157-168. https://doi.org/10.1007/s10661-006-2525-z

Seed, R. B., Cetin, K. O., Moss, R. E. S., Kammerer, A., Wu, J., Pestana, J., Riemer, M., Sancio, R. B., Bray, J. D., Kayen, R. E., and Faris, A. Recent advances in soil liquefaction engineering: A unified and consistent framework. Keynote presentation, 26th Annual ASCE Los Angeles Geotechnical Spring Seminar 2003, Long Beach, CA.

Seed HB and Idriss IM. Simplified procedure for evaluating soil liquefaction. Journal of Soil Mechanics and Founddation Division 1971;97(9):1249–1273. https:// doi. org/ 10. 1061/ JSFEAQ. 00016 62.

Tsuchida H. Prediction and countermeasure against the liquefaction in sand deposits. Abstract of the Seminar in the Port and Harbor Research Institute 1970 (in Japanese).

Yuce, G., D'Alessandro, W., Yalcin, T., Yasin, D., Gulbay, A., Ozyurt, N., Rojay, B., Karabacak, V., Bellomo, S., Brusca, L., Yang, T., Fu, C., Lai, C., Özacar, A. & Walia, V. Origin and interactions of fluids circulating over the Amik Basin (Hatay, Turkey) and relationships with the hydrologic, geologic and tectonic settings. Chemical Geology 2014;388:23-39. https://doi.org/10.1016/j.chemgeo.2014.09.006.